

## Creep and Tensile Properties of Direct Metal Laser Sintered (DMLS) Inconel 738LC Coupons and Comparison to Cast Properties

Jason Wilkes, Ph.D.  
Southwest Research Institute  
San Antonio, TX  
[jason.wilkes@swri.org](mailto:jason.wilkes@swri.org)

Kevin Hoopes  
Southwest Research Institute  
San Antonio, TX  
[kevin.hoopes@swri.org](mailto:kevin.hoopes@swri.org)

John Helfand  
Southwest Research Institute  
San Antonio, TX  
[john.helfand@swri.org](mailto:john.helfand@swri.org)

*Dr. Jason Wilkes is a Senior Research Engineer in the Rotating Machinery Dynamics Section at Southwest Research Institute in San Antonio, TX. His experience at SwRI includes design and construction of various test rigs and machine prototypes, predicting lateral and torsional rotordynamic analyses, bearing and seal design and application, and auxiliary bearing dynamics following failure of AMB supported turbomachinery. Dr. Wilkes holds a B.S., M.S., and Ph.D. in Mechanical Engineering from Texas A&M University where he worked at the Turbomachinery Laboratory for 6 years*

### ABSTRACT

Due to the nature of sCO<sub>2</sub> power cycles, a number of turbine parts must have good mechanical properties at elevated temperatures. For recompression cycles, the turbine inlet temperature is between 600°C - 750°C, which puts nearly all high-temperature turbine parts into a creep regime. The high-strength parts in these applications are often composed of materials having high nickel or chrome contents, and are often termed superalloys. At these temperatures, the blades must survive mechanical loads due to centrifugal stress and blade loading. While centrifugal stress is primarily a function of tip velocity and its associated centrifugal acceleration, blade loading is a function of power density. Since sCO<sub>2</sub> turbomachinery is approaching the power density of rocket engines, blade loading tends to be quite large. Another result of this high power density is that blade passages for 1-10 MW turbines tend to be quite small, making conventional fabrication methods challenging and costly; this leads engineers to pioneer new techniques to address these challenges. The authors of the current work are addressing this challenge by applying additive manufacturing techniques in the production of a 10 MW radial inflow impeller.

While a comprehensive database exists for the mechanical properties of forged and cast superalloys, data is sparse for superalloys fashioned by direct metal laser sintering (DMLS) or other additive manufacturing methods. For the remainder of this work, the term printed will refer to components manufactured using one of these processes for brevity. The current work stems from the desire to manufacture a radial inflow turbine impeller using additive manufactured (AM) Inconel 738. While Siemens has adopted the use of DMLS printed Inconel 738 for use in select aviation engine parts, creep and tensile properties have not been published to the extent needed to validate a given design. The current work will show creep and tensile properties of AM Inconel 738 in the horizontal and vertical build directions and their respective comparison to cast Inconel 738 properties.

### INTRODUCTION

Due to its unique fluid properties, sCO<sub>2</sub> power cycles have the ability to outperform traditional steam and organic Rankine power cycles in terms of overall cycle efficiency as well as machinery complexity and compactness. To advance the state of the art in sCO<sub>2</sub> turbomachinery, Southwest Research Institute and Hanwha Power Systems Americas, were awarded a project funded by the U.S. Department of Energy SunShot Initiative to develop an integrally geared compander for use in concentrated solar power (CSP) sCO<sub>2</sub> plant applications. This effort focused on the optimization of the overall thermodynamic cycle as well as the detailed design, development, and testing of critical turbomachinery components [1-5]. Currently the project is finishing the detailed design phase with manufacturing and testing scheduled to occur in 2018/2019.

The design of the radial turbine for the integrally geared compander required it to be manufactured using Inconel 738 and with an additive manufacturing process. This process will allow for a shroud cover which increases the overall cycle efficiency and also allow for axial shaft growth. Due to the high turbine inlet temperature dictated by the cycle conditions, the turbine life will be governed by the materials resistance to creep which is why Inconel 738 was chosen.

This paper presents the results of a test program to investigate the effect of additive manufacturing on creep rupture life of Inconel 738 test samples.

## **LITERATURE REVIEW**

Inconel 738 was developed by the International Nickel Company in the late 1960s [6]. Since its introduction, it has been used extensively in high temperature environments typical of jet engine applications. These environments rely on the high temperature creep rupture strength of Inconel 738. High temperature material property data, including creep rupture strength, for cast Inconel 738 is widely available in the literature, [7,8].

Rickenbacher [9] and Kunze [10] present the first look at high temperature creep rupture strength of additively manufactured Inconel 738 in comparison to the cast material properties. These results show that additively manufactured Inconel 738 shows reduced creep rupture strength when compared to cast specimens as well as significant anisotropy. In their study, the creep rupture strength is greatly reduced when the specimen was stressed along build layers. The authors of these studies conclude that the superior creep rupture strength in the samples that were stressed in a direction perpendicular to the build layers was due to “columnar elongated grains” which exhibit increased creep rupture strength in a similar manner as single crystal cast superalloys routinely used in cast turbine blades.

The present work extends the previous investigations into AM Inconel 738 creep properties by providing additional tests at different stresses and temperatures as well as testing specimens at stresses and temperatures relevant to an upcoming sCO<sub>2</sub> turbine test. Also due to variability of the AM process from vendor to vendor the current sCO<sub>2</sub> test program required the additional creep life testing presented in this work to help qualify the vendor.

## **BACKGROUND**

The samples in this study were printed from Inconel 738LC by Materials Solutions in the UK. For more information on the Inconel 738LC please see Appendix 1 or the referenced INCO bulletin [7]. The “LC” in Inconel 738LC stands for low carbon. The reason that this version of Inconel 738 was developed was to improve castability in large parts over its standard Inconel 738 counterpart. Additionally castability was also improved by reducing Zirconium in the LC version. Following the printing process the materials went through a hot-isostatic press process to help seal any internal voids, then the material was heat treated. As is certainly undesirable to the reader, the heat treat process used for these samples was proprietary to Materials Solutions, and therefore it was not shared with the authors; however, the authors understanding is that a standard cast Inconel 738LC heat treatment was used. The material samples were then machined per ASTM E139 similar to the sample shown in Figure 1.

To completely characterize printed Inconel 738 LC would require a substantial amount of time and money. While creep tests are generally costly, characterizing printed Inconel 738 samples is even more costly because the average cost for each sample is approximately 1,000 USD. Since complete material characterization is well beyond the scope of the current development, a test sequence was designed to yield the most value to the current effort.



**Figure 1: Example specimen profile and associated creep elongation calculation**

Figure 2 shows test data for cast Inconel 738 along with select test points that are accented by green highlights. These points were selected for two reasons: (1) the green dots provide strain and rupture data that are directly comparable to cast properties, which allows for a generalized comparison between creep properties for printed and cast materials that is useful to a wider audience; and (2) the initial impeller design stress that was used in the current effort was approximately 40-60 ksi depending on material temperature. This design stress was taken from the cast properties shown below at design temperatures for the current project. Selecting a test stress in this range allows Larson Miller Parameter (LMP) scaling to apply to the test data to determine applicable design stresses as a function of design life and temperature. This notion is observed from Swaminathan and Lowden, who note that “for reliable life estimates, then, accelerated test conditions must be selected such that the creep damage process occurring is identical to that under service conditions. For materials where creep damage results primarily from thermally induced changes in microstructure, temperature acceleration should be adopted in preference to stress acceleration. It is well established that stress acceleration is not applicable to nickel base superalloys, however, if it is used, the resulting projections will be conservative.” [12]. Swaminathan also notes that creep data can only be extracted out to about 3 times the duration of the test data. While we will be exceeding this rule of thumb, time and budget did not permit a 33,000 hour test to be completed to evaluate 100,000 hour service life.

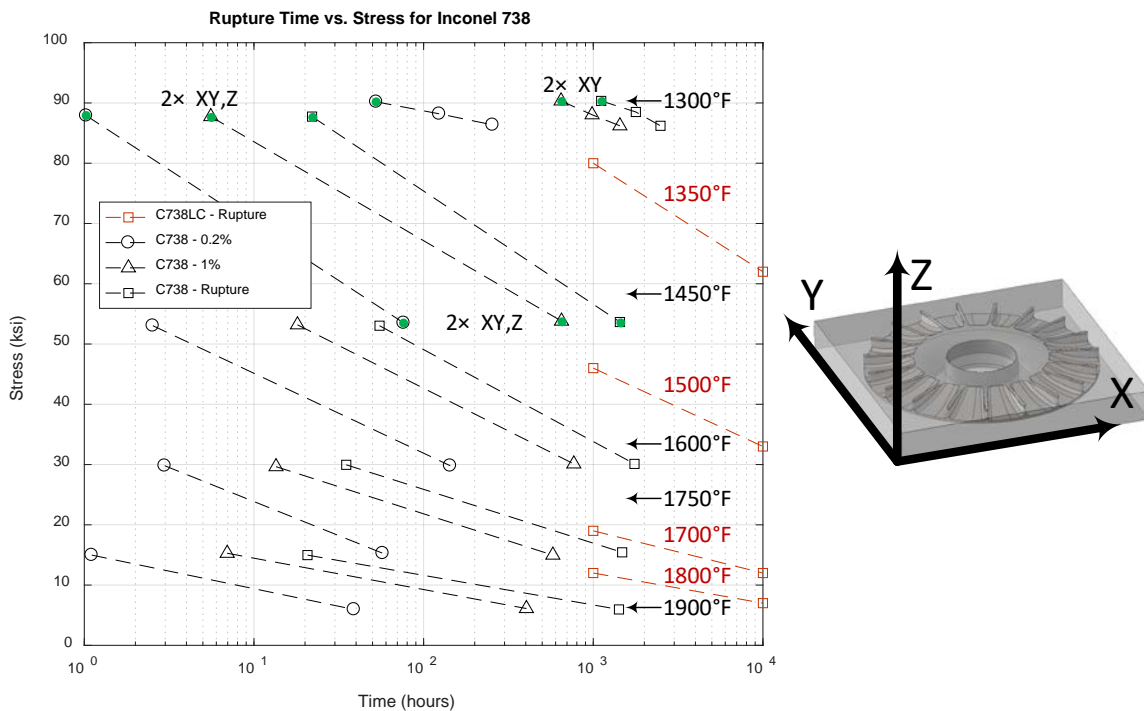


**Figure 2: Cast Inconel 738 Creep Sample Data and Associated Test Points (Denoted by Green Accent), Heat Treat - 2050F, 2 hrs, AC +1550F, 24 hrs, AC (data taken from [8])**

Samples tested in this program included 6 samples in the XY orientation and 4 samples in the Z orientation as illustrated in Figure 2. Two identical XY samples were tested each of the three design conditions shown, while only the 1450°F test points were evaluated using samples in the Z orientation. Unfortunately due to miscommunication with the AM vendor, it was not understood that the printed samples were Inconel 738LC until after creep testing had been performed; however, the only source of data for cast Inconel 738LC were at conditions that were substantially longer as shown, which would have been cost prohibitive. As such, comparisons will be made to cast Inconel 738 and Inconel 738LC; however only a direct comparison to the cast Inconel 738 temperatures is permitted.

## RESULTS AND DISCUSSION

Figure 2 shows a compilation of creep rupture stress vs. time from a variety of sources. These sources include data from the aerospace materials handbook at relevant temperatures shown in Figure 2, the creep data obtained during this study from printed materials samples, as well as data from printed Inconel 738LC as provided in Rickenbacher et al. and Kunze et al. [9, 10].

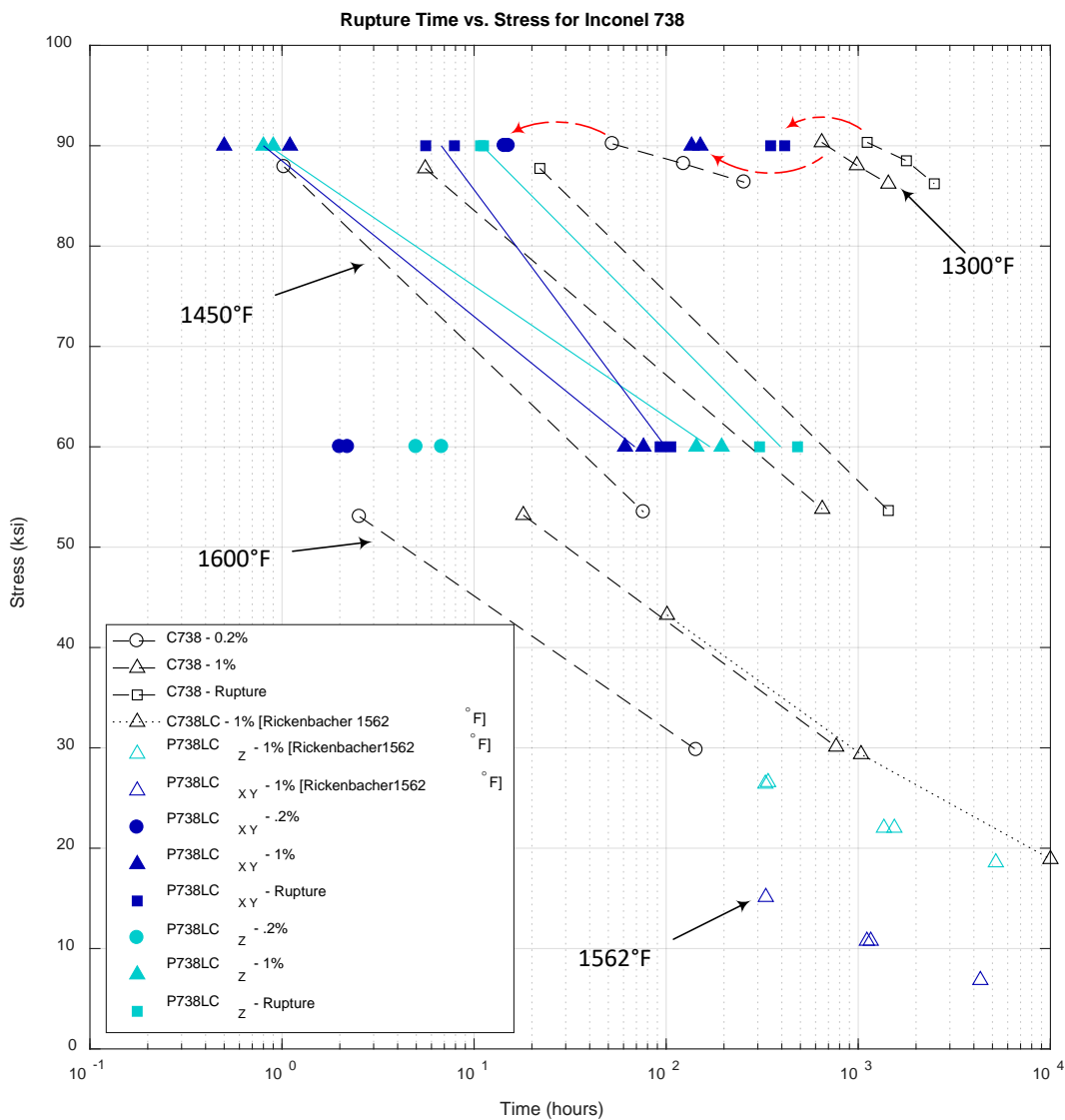


**Figure 3: Rupture Time vs. Stress for Various Inconel 738 and Inconel 738LC Samples**

While the authors apologize for the sheer volume of data in this plot, it is important that these data are all

viewed on the same graph. Starting first with a description for the conventions used in the plot, the following holds in each of the remaining plots unless otherwise stated. The shape of the symbols denotes the amount of strain. Circles denote a strain of 0.2%, triangles denote a strain of 1%, and squares denote that the sample is ruptured. Colors represent the source of the data. Black denotes data obtained from cast samples, which is denoted by C738 in the legend of each figure. Dark blue and light blue colors represent AM (or printed) samples data in the XY (P738LC<sub>xy</sub>) and Z (P738LC<sub>z</sub>) orientation, respectively. Once again, the XY samples are stressed along horizontal plane shown in the diagram in Figure 2, while the Z samples are stressed along the vertical Z axis. Additionally, the solid blue shapes represent samples tested during this test campaign, while hollow symbols represent printed samples obtained from the literature.

Observe first the direct comparison between printed samples and cast Inconel 738 at 1300°F as highlighted by the red arrows. It is immediately apparent that at 1300°F and at 90 ksi that the printed samples failed at substantially shorter duration than the cast samples. Note that these samples were oriented in the XY frame; that is, they were stretched along build layers. This trend also holds at 1450°F as well for printed XY samples; however, this figure clearly shows that the samples in the Z orientation outperform the XY samples in creep. In fact, they are approaching the cast properties in behavior. These results match the findings by Rickenbacher et al. who also showed strong anisotropic behavior for SLM samples.

While these results are useful comparatively, it is difficult to directly employ this data in the design of turbomachinery components. To this end, Larson and Miller came up with a formula to define creep behavior relative to a modified time-temperature parameter [13]. This parameter is known as the Larson Miller Parameter (LMP). The form employed for this analysis is

$$LMP = T(C + \log_{10} t) / 1000, \quad (1)$$

where  $T$  is the temperature in absolute units (Rankine),  $C$  is a constant (20 employed in this work), and  $t$  is the time of rupture. Using this parameter, the time and temperature data can be normalized as shown in Figure 4. Note here that LMP has been divided by 1000 to provide data at a more favorable scale. This figure shows all of the cast rupture data shown in Figure 2 from [8,14] along with the rupture data from all 10 creep samples tested during this effort.

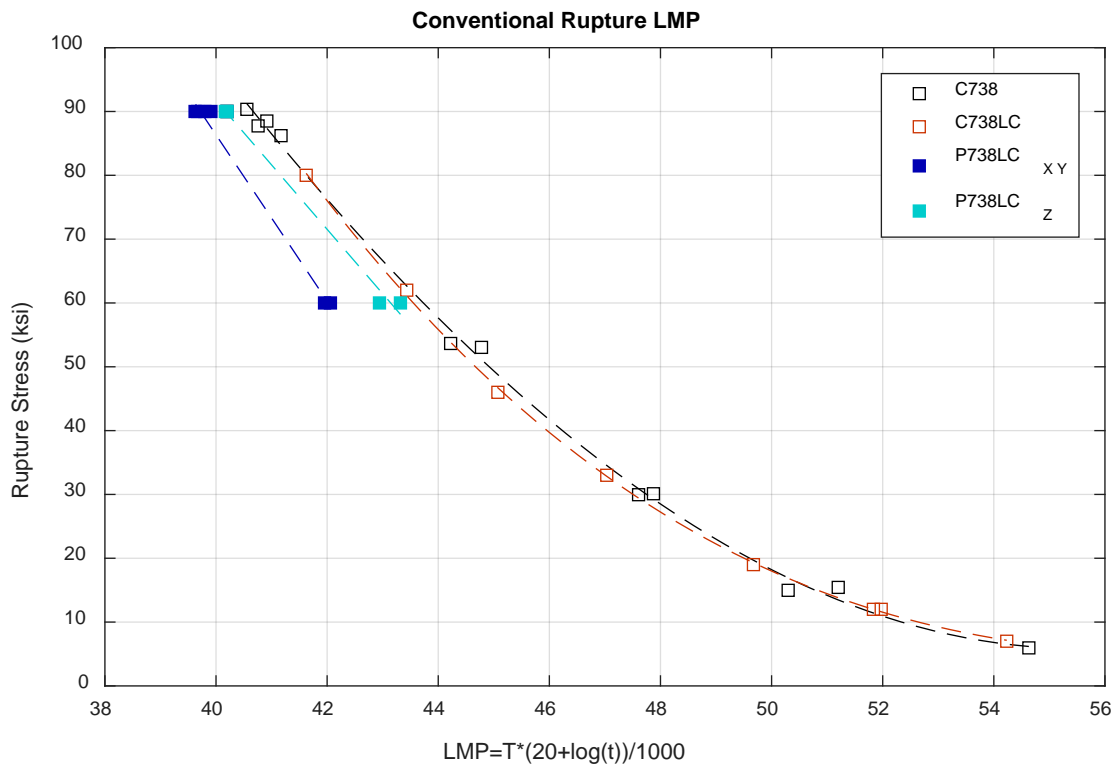


Figure 4: Stress vs. Conventional LMP for Samples at Rupture

Figure 4 suggests that the creep-rupture properties of cast Inconel 738 and cast Inconel 738LC are actually very similar according to the data obtained. This implies that the comparisons between cast Inconel 738 and additively manufactured Inconel 738LC can likely be generalized, and time will tell whether these trends hold for other alloys in creep.

In addition to the data shown, these terms have been fit such that at a given desired design life/temperature, the rupture stress can be calculated. Note that due to the limited number of stress levels tested in this campaign, a linear fit of stress vs. LMP was used for the test data, while a higher order function was used to fit the cast data. While it may seem likely that the printed coupons would have similar behavior at elevated LMP as demonstrated by the cast material shown in Figure 4, it can be observed that stress at higher LMP would be conservative. For the sake of completeness, let us assume that this data would be used to determine an acceptable design stress for an impeller with a hoop stress in the XY orientation at a mean temperature of 1300F. Note that the desired life is 100,000 hrs. In this case, the LMP for this condition can be calculated as

$$LMP = (1300 + 459.7) \left[ 20 + \log_{10} (100,000) \right] / 1000 = 43.99 \quad (2)$$

From Figure 4, extrapolating out to an LMP of 44, it appears that the sample would rupture at approximately 32 ksi. Although it may not be completely applicable for an impeller, the ASME Boiler and Pressure Vessel Code defines allowable design stress in creep as the average rupture stress with a 1.5 safety factor. Therefore, the allowable stress in this case would be 21.4 ksi.

Another parameter that can be used to reduce the data is to use a modified strain based LMP formulation

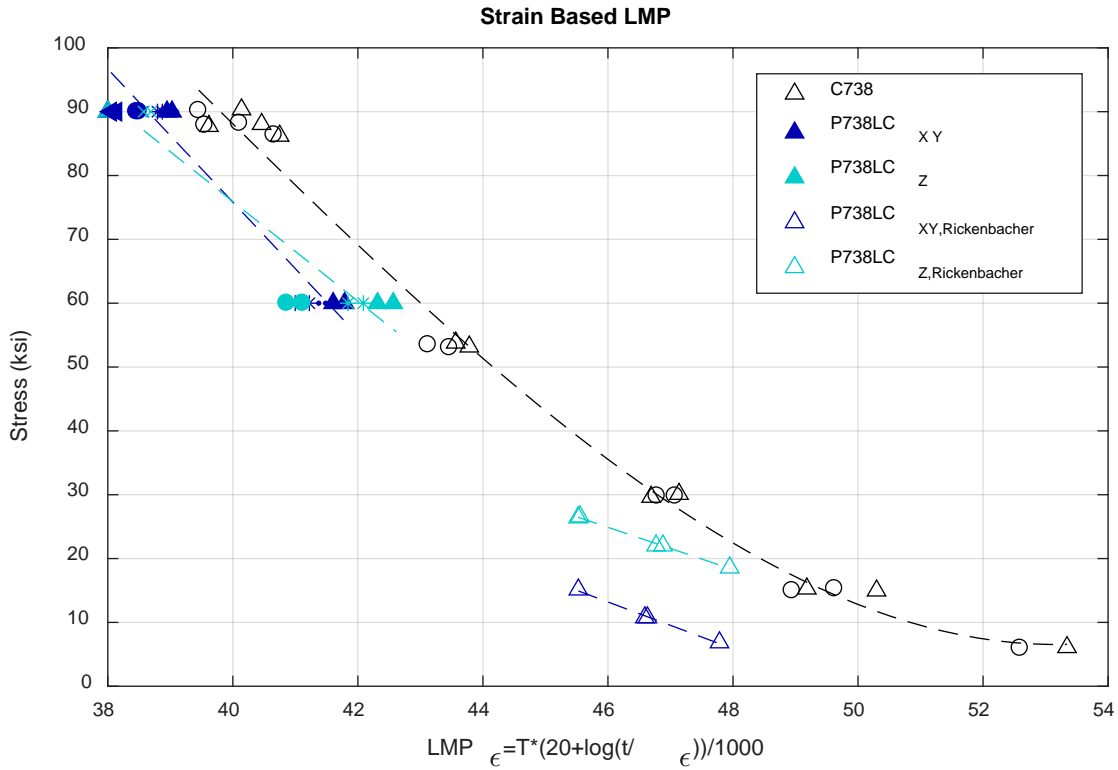
$$LMP_{\varepsilon} = T \left[ C + \log_{10} \left( \frac{t}{\varepsilon} \right) \right] / 1000 \quad (3)$$

This form is useful for bolt calculations where creep behavior changes the stress on the bolt (creep relaxation) or for designs where a specific allowable creep elongation target is established. Swaminathan also notes that cracks initiate at strains below 1%, and that a strain target may be a more suitable criteria for design[12].

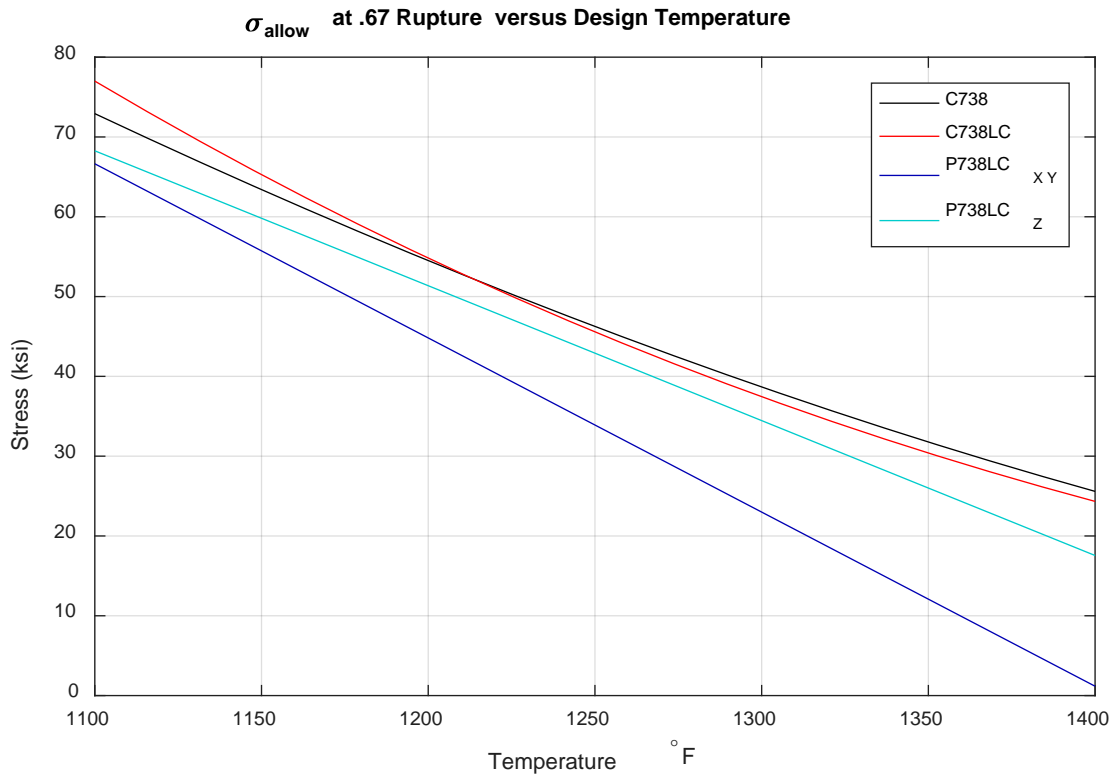
Figure 5 shows the modified strain based LMP for the cast samples, the printed samples obtained in this project, and those taken from the literature. This figure similarly shows that the allowable stress for printed Inconel 738 is lower in the XY orientation than it is in the Z orientation. Although the strain based data taken in this report does not seem definitive at a  $LMP_{\varepsilon}$  less than 39.5, the crossover point shown in Figure 5 where the printed XY coupon is stronger than the Z coupon is at a stress approaching yield, where low cycle fatigue would be a concern. Due to the difference in slope however, it is clear that at higher LMP, the Z sample will outperform the XY sample. Although not specifically included in the caption for clarity, the other symbols in the chart denote different strains; in this figure, Circles denote 0.2% strain, asterisks denote 0.5% strain, and triangles denote 1% strain.

Figure 6/Table 1 shows the allowable design stress for 100,000hr operation for the various coupons assuming that a 1.5 safety factor relative to rupture is used, while Figure 7 and Table 2 show similar results for 100,000hr life targeting a mean strain of 0.2%. In turbomachinery, designers must take care to ensure that excessive rotor-stator contact is avoided. A strain of 0.2% on an 8" diameter wheel is approximately 0.008 in of radial creep. In sCO<sub>2</sub> turbomachinery, this is certainly on-the-order of the seal clearances. Although the entire wheel may not creep 0.2% this is a conservative value that can be used to bound the design.

This data shows that the creep strength of Inconel 738 in a printed orientation falls off dramatically above 1100 F. Below 1100F, it is likely that low-cycle fatigue would be the likely failure mechanism of the material.



**Figure 5: Stress vs. Strain Based LMP**



**Figure 6: Allowable Stress for 100,000 hr Design Life vs. Design Temperature at 1.5 Safety Factor to Rupture**

**Table 1: Allowable Stress (ksi) for 100,000 hr Design Life vs. Design Temperature at 1.5 Safety Factor to Rupture**

Temperature (°F)	1100	1200	1300	1400
C738	72.9	54.5	38.7	25.6
C738LC	77.0	54.8	37.4	24.3
P738LC <sub>XY</sub>	66.6	44.8	23.0	1.2
P738LC <sub>Z</sub>	68.3	51.4	34.5	17.6

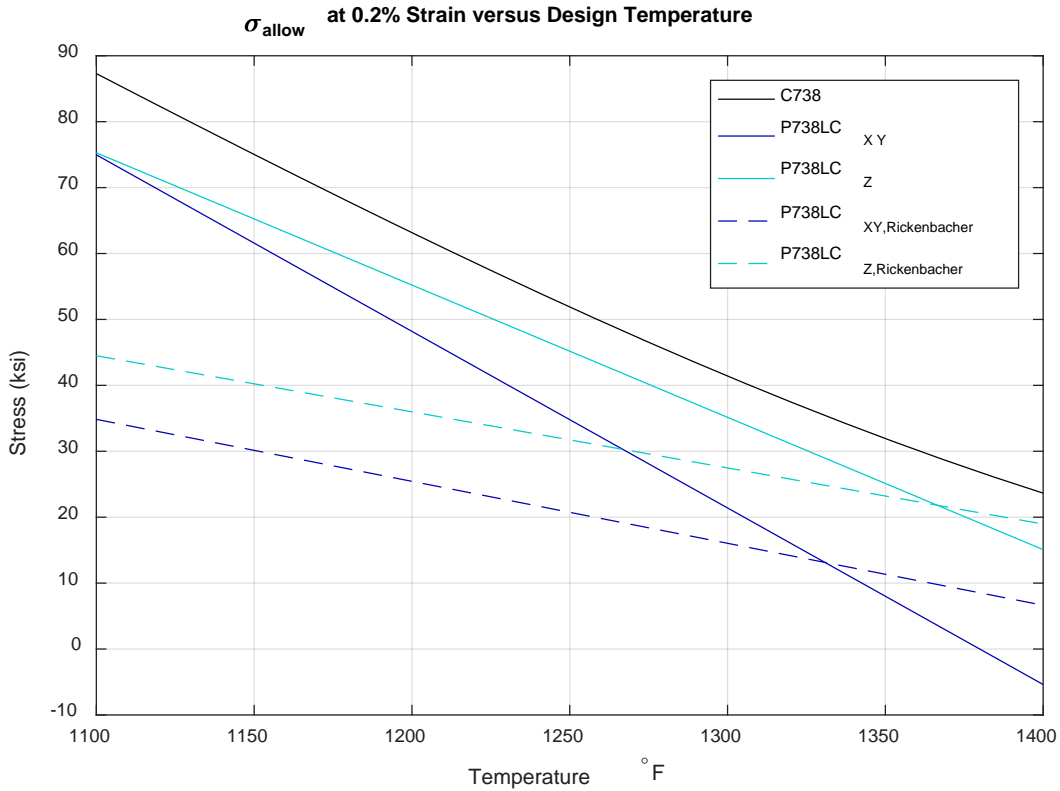


**Figure 7: Allowable Stress vs. Design Temperature at 0.2% Strain**

**Table 2: Allowable Stress (ksi) for 100,000 hr Design Life vs. Design Temperature at 0.2% Strain**

Temperature (°F)	1100	1200	1300	1400
C738	87.3	63.2	41.4	23.6
P738LC <sub>XY</sub>	75.0	48.2	21.4	0.0
P738LC <sub>Z</sub>	75.3	55.2	35.1	15.1
P738LC <sub>XY,Rickenbacher</sub>	34.8	25.4	16.0	6.6
P738LC <sub>Z,Rickenbacher</sub>	44.5	36.0	27.5	19.0

In addition to creep properties at elevated temperatures, elevated temperature tensile tests were also performed at 1100°F and 1300°F. These results are shown in Figure 8. These results show that the yield strength in both orientations is lower than cast properties; however, the ultimate tensile strength of both



samples is quite high. This suggests that the material is quite ductile as evidenced by the elongation of 15-24% as detailed in Table 3.

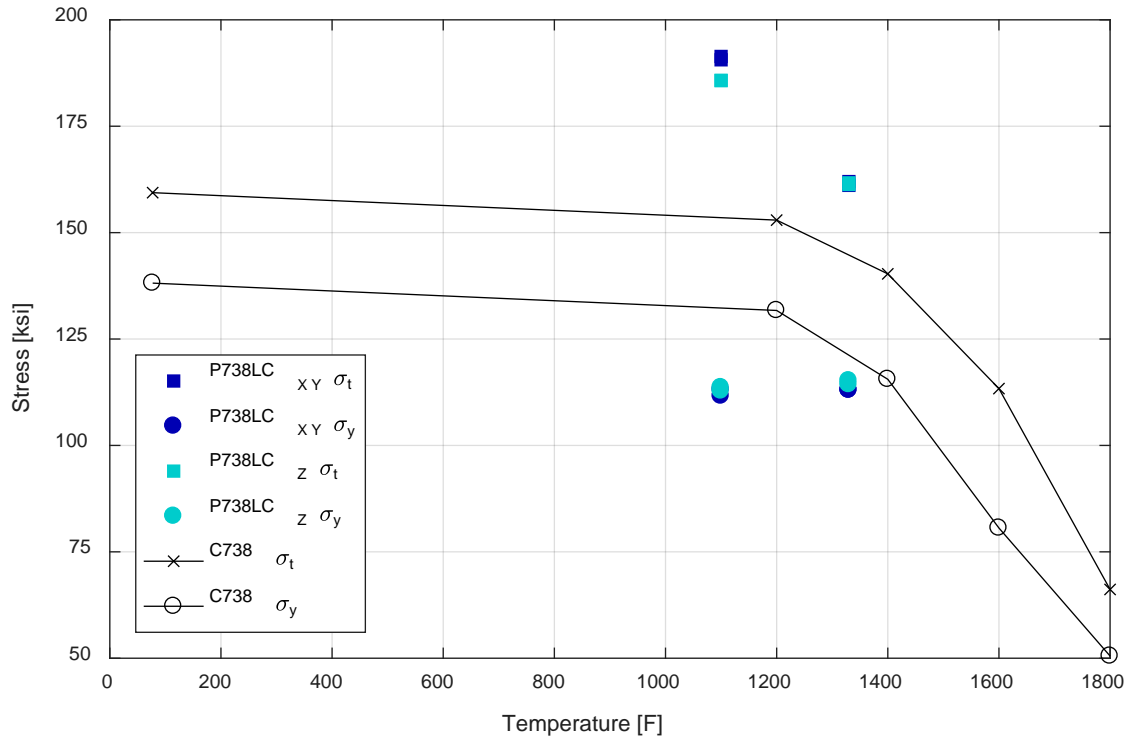


**Figure 8: High-Temperature Tensile and Yield Stress**

**Table 3: Tensile Test Data for Inconel 738LC at Elevated Temperatures (S denotes samples aligned with the XY plane, and R denotes samples aligned with the Z axis)**

Specimen ID	Test Temper	Diameter (Inches)	Ultimate Strength	Yield Strength	Elongation (%)	Reduction Of Area (%)	Fracture Location
S1	1330	0.2507	162,000	113,000	17.5	27.1	Gage
S2	1330	0.2493	161,100	113,000	16.8	23.9	Gage
S3	1100	0.2498	190,600	111,600	15.4	23.5	Gage
S4	1100	0.2496	191,400	113,100	15.6	22	Gage
R1	1330	0.2507	161,300	114,300	21.6	34.1	Gage
R2	1330	0.2507	161,700	115,200	23.4	37.3	Gage
R3	1100	0.2509	185,800	113,600	15.2	23.1	Gage
R4	1100	0.251	185,700	112,800	14.6	22.1	Gage

As a final note, Figure 9 shows residual creep occurring in an example impeller wheel after 100,000 hours of operation. This figure results from an elastic perfectly-plastic material model with allowable stresses corresponding to those shown in the XY orientation in Figure 6. Note that the diameter and speed of this wheel approximate those used in the actual design. Additionally, this model includes thermal and pressure loads that give rise to accurate temperature profiles in the wheel such that creep strength throughout the wheel is well approximated. These loads were imported from a separate conjugate heat transfer analysis. As per elastic-plastic analysis in the ASME Boiler and Pressure Vessel Code, Section 8-DivII, this impeller would qualify in creep [15].

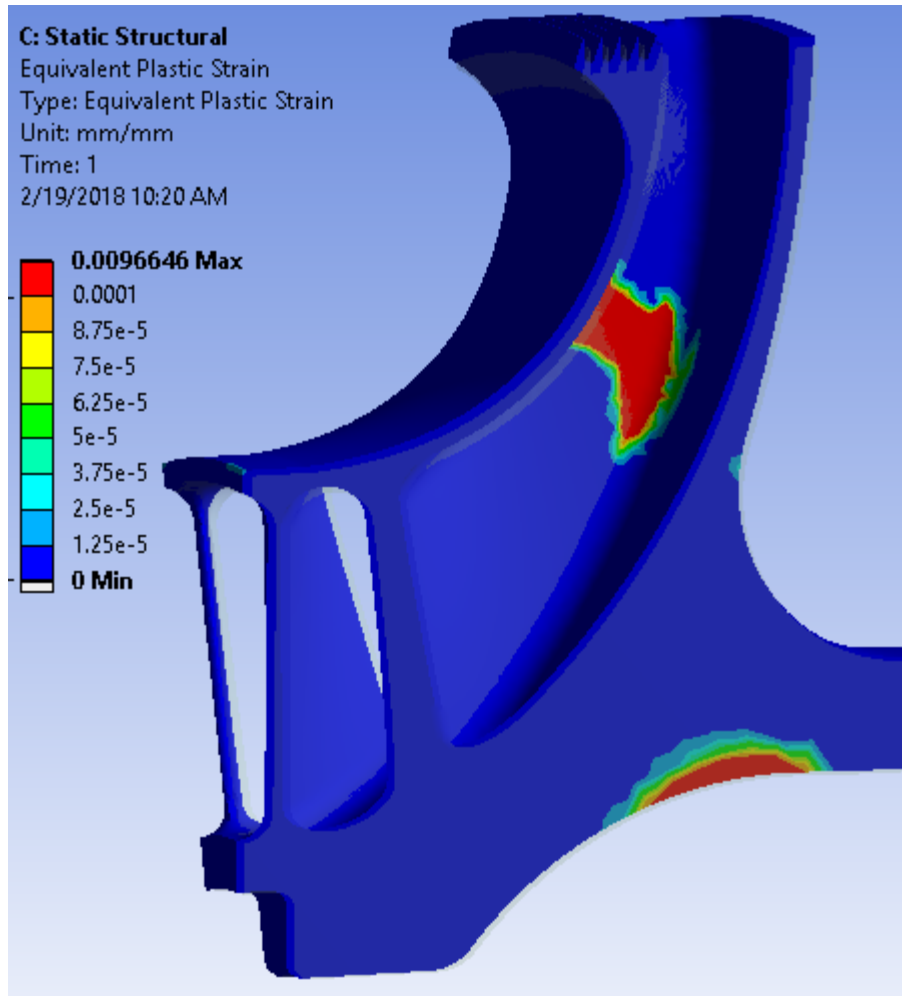


**Figure 9: Permanent Strain due to Creep Deformation after 100,000 Hours of Service**

## CONCLUSIONS

This paper presents results for creep behavior of printed Inconel 738LC test specimens as compared to Inconel 738 cast properties. While minimal data previously existed in the literature, the current work expands on the available data and presents design guidelines for use in sCO<sub>2</sub> design. In general, the results found in this paper corroborate the conclusions by Rickenbacher. Namely, the creep strength of the additively manufactured specimens is in general weaker than corresponding cast specimens, and creep strength falls off faster at elevated temperature than corresponding cast samples. Additionally, the creep strength normal to build layers is superior to the creep strength oriented along a build layer. Although this discrepancy is minor at 1100-1150°F, it becomes quite pronounced at increased temperatures. At 1200°F and 1300°F, the XY rupture strength is approximately 87% and 67% of the rupture strength along the Z orientation. This is again relative to samples normal to the build that are in general 5-10% weaker than cast properties up to 1300°F. Above this temperature, even printed coupons in the Z axis fall off dramatically. Even with these shortcomings, Figure 9 demonstrates that the printed Inconel 738LC has sufficient creep strength to survive 100,000 hour service life in sCO<sub>2</sub>.

## ACKNOWLEDGEMENTS

This material is based upon work supported by the Department of Energy, Office of Energy Efficiency and Renewable Energy (EERE), under Award Number DE-0007114. The authors would also like to acknowledge materials solutions for providing the samples for this test program. Additionally, this project

would not be possible without the help and support of our cost-share provider and project partner Hanwha Power Systems America. Specifically, Karl Wygant, Rob Pelton, Jon Bygrave, have been instrumental in this undertaking.

## REFERENCES

- [1] Wilkes, J., Allison, T., Schmitt, J., Bennett, J., Wygant, K., Pelton, R., Bosen, W., 2016, "Application of an Integrally Geared Comander to an SCO<sub>2</sub> Recompression Brayton Cycle," *Proc. 5<sup>th</sup> Intl. Symp. – Supercritical CO<sub>2</sub> Power Cycles*, March 28-31, San Antonio, TX.
- [2] Wilkes, J., Allison, T., 2016, "Development of an Ultra-High Efficiency Wide-Range Integrally-Geared Supercritical CO<sub>2</sub> Comander," *Concentrating Solar Power Program Summit*, April 19-20, San Diego, CA.
- [3] Wilkes, J., Bennett, J., Schmitt, J., Wygant, K., and Pelton, R., 2017, "Application of an Integrally Geared Comander to an SCO<sub>2</sub> Recompression Brayton Cycle," *Proc. of 1<sup>st</sup> Global Power and Propulsion Forum*, Paper GPPF-2017-166, January 16-18, Zurich, Switzerland.
- [4] Bennett, J., Wilkes, J., Allison, T., Wygant, K., and Pelton, R., "Cycle Modeling and Optimization of an Integrally Geared sCO<sub>2</sub> Comander," *Proc. of ASME Turbo Expo 2017*, Paper GT2017-63707, June 26-30, Charlotte, NC.
- [5] Schmitt, J., Wilkes, J., Allison, T., Bennett, J., Wygant, K., and Pelton, R., "Lowering the Levelized Cost of Electricity of a Concentrating Solar Power Tower with a Supercritical Carbon Dioxide Power Cycle," *Proc. of ASME Turbo Expo 2017*, Paper GT2017-64598, June 26-30, Charlotte, NC.
- [6] US patent, (<https://www.google.com/patents/US3459545>)
- [7] Alloy IN-738 technical data ([http://www.nipera.org/~Media/Files/TechnicalLiterature/IN\\_738Alloy\\_PreliminaryData\\_497\\_.pdf](http://www.nipera.org/~Media/Files/TechnicalLiterature/IN_738Alloy_PreliminaryData_497_.pdf))
- [8] Aerospace Metals Handbook
- [9] Rickenbacher, L., Etter, L., Hovel, S., and Wegener, K., 2013, "High temperature material properties of IN738LC processed by selective laser melting (SLM) technology," *Rapid Prototyping Journal*, DOI 10.1108/13552541311323281.
- [10] Kunze, K., Etter, T., Grasslin, J., Shklover, V., 2014, "Texture, anisotropy in microstructure and mechanical properties of IN738LC alloy processed by selective laser melting (SLM)," *Journal of Materials Science and Engineering*.
- [11] ASME Standard ASTM E139-11 "Standard Test Methods for Conducting Creep, Creep-Rupture, and Stress-Rupture Tests of Metallic Materials"
- [12] Swaminathan, V. P., and Lowden, P., 1989, "Gas Turbine Blade Life Assessment and Repair Guide," GS-6544 Research Project 2775-6.
- [13] Larson, F. and Miller, J., "A Time-temperature Relationship for Rupture and Creep Stresses," *Transactions of the ASME*, July 1952, pp. 765-775.
- [14] The International Nickel Company Inc., "Alloy IN-738 Technical Data"
- [15] American Society of Mechanical Engineers. 1900. *ASME boiler and pressure vessel code*. New York: [American Society of Mechanical Engineers, Boiler and Pressure Vessel Committee].

**APPENDIX 1: INCONEL 738LC CHEMICAL COMPOSITION**

**TABLE I**  
**Composition of Alloy IN-738**

Element	Composition, weight percent			
	High Carbon IN-738C		Low Carbon, Low Zirconium IN-738LC	
	Range	Nominal	Range	Nominal
Carbon	0.15-0.20	0.17	0.09-0.13	0.11
Cobalt	8.00-9.00	8.50	3.00-9.00	8.50
Chromium	15.70-16.30	16.00	15.70-16.30	16.00
Molybdenum	1.50-2.00	1.75	1.50-2.00	1.75
Tungsten	2.40-2.80	2.60	2.40-2.80	2.60
Tantalum	1.50-2.00	1.75	1.50-2.00	1.75
Columbium (Niobium)	0.60-1.10	0.90	0.60-1.10	0.90
Aluminum	3.20-3.70	3.40	3.20-3.70	3.40
Titanium	3.20-3.70	3.40	3.20-3.70	3.40
Aluminum + Titanium	6.50-7.20	6.80	6.50-7.20	6.80
Boron	0.005-0.015	0.010	0.007-0.012	0.010
Zirconium	0.05-0.15	0.10	0.03-0.08	0.05
Iron	0.05 max	LAP <sup>†</sup>	0.05 max	LAP <sup>†</sup>
Manganese	0.02 max	LAP	0.02 max	LAP
Silicon	0.30 max	LAP	0.30 max	LAP
Sulfur	0.015 max	LAP	0.015 max	LAP
Nickel	Balance	Balance (61)	Balance	Balance (61)

† Low as possible

\* U.S. Patent #3,459,545, produced under license from  
The International Nickel Company, Inc.